Sonoelastography of parotid gland tumours: initial experience and identification of characteristic patterns

Nils Klintworth · Konstantinos Mantsopoulos · Johannes Zenk · Georgios Psychogios · Heinrich Iro · Alessandro Bozzato

Abstract

Objectives The aim of this study was to investigate B-mode and elastographical ultrasound criteria capable of differentiating between benign and malignant parotid tumours and to define characteristic elastographical patterns for pleomorphic adenomas and Warthin's tumours.

Methods Fifty-seven patients with parotid gland tumours were examined using a combination of B-mode and elastographic ultrasounds. The data acquired were analysed retrospectively by two experienced ultrasound operators to identify specific sonographical features of benign and malignant lesions. Additionally, elastographical patterns were defined and analysed for their specificity.

Results A blurred margin proved to be the only significant criterion in B-mode ultrasound capable of differentiating between malignant and benign tumours. The garland sign was defined as an elastographical pattern found significantly more frequently in malignant tumours, improving sonographical prediction of the benign or malignant nature of a parotid lesion. A logistic regression model was developed that achieved a correct prediction in 87.7% of cases. A "dense core" sign was also specifically defined for pleomorphic adenomas and a "half-half" sign for Warthin's tumours.

Conclusions Elastography is an innovative and powerful diagnostic tool that can improve the sonographical examination of parotid gland tumours by revealing easily recognised and characteristic patterns of tissue distribution.

N. Klintworth (✉) · K. Mantsopoulos · J. Zenk · G. Psychogios · H. Iro · A. Bozzato
Department of Otorhinolaryngology, Head and Neck Surgery, University of Erlangen-Nuremberg,
Waldstrasse 1,
91054 Erlangen, Germany
e-mail: nils.klintworth@uk-erlangen.de

Key Points

- *Elastography can help differentiate benign from malignant parotid tumours during parotid ultrasound.*
- *The elastographical "garland sign" is more frequent in malignant than benign parotid tumours.*
- *Pleomorphic adenomas show an elastographical "dense core sign".*
- *Warthin's tumours show an elastographical "half-half sign".*
- *Parotid cysts show an elastographical "bull's-eye sign".*

Introduction

Preoperative assessment of the benign or malignant nature of parotid tumours needs to be as precise and reliable as possible. The extensiveness and urgency of the surgical procedures required differ: while a presumably benign lesion can be removed using a lateral parotidectomy or a less invasive technique (e.g. extracapsular dissection), total or even radical parotidectomy combined with neck dissection has to be urgently planned if there is any suspicion of malignancy [1, 2].

However, the signs and symptoms of parotid gland tumours are often nonspecific [3]. Preoperative cytological examination using fine-needle aspiration can improve the diagnostic accuracy, but the reliability of cytology findings may be questionable, as false–negative and false–positive results are possible even when the biopsy is carried out with ultrasound guidance [4, 5].

Imaging techniques therefore play a crucial role in the preoperative assessment of parotid gland tumours. High-

resolution ultrasound is a well-accepted method in this context. It is able to depict the exact location and size of tumours in the majority of cases, as most lesions are located superficially and are thus easily accessible [6–8]. Additionally, computed tomography (CT) and magnetic resonance imaging (MRI) in particular can provide further detailed information with regard to the relationship between the tumour and the surrounding soft tissue (MRI) or bony structures such as the mandible or temporal bones (CT) [9, 10].

Efforts to develop an imaging technique that would be capable of differentiating between benign and malignant lesions have been reported in numerous studies [11–13]. In recent years, MRI has achieved promising results here; diffusion-weighted sequences in particular have provided remarkably good results, with sensitivity and specificity rates of 85–95% being reported for differentiating between benign and malignant parotid tumours [14–16].

The question arises of whether ultrasonography, as an easily available, cost-effective and harmless technique (with no radiation exposure and no need for contrast agent administration) can achieve comparable results. Several criteria for distinguishing between benign and malignant lesions are well established in ultrasound examinations of parotid tumours. For example, benign tumours present with regular and sharp margins, a homogeneous hypoechoic texture and defined perfusion (e.g. central or peripheral), whereas malignancies lack these characteristics and are irregular, heterogeneous and diffusely perfused [17–19]. However, these features overlap broadly within the histological heterogeneous group of parotid lesions, and many benign tumours—above all pleomorphic adenomas—appear as irregularly shaped, heterogeneous lesions that cannot be distinguished from malignancies. This poses a challenge even for experienced ultrasound operators attempting to classify the specific type of lesion or to predict a lesion's malignancy with a satisfactory level of confidence.

Additional ultrasound applications may improve the reliability of tumour differentiation. Some differences in flow kinetics have been observed between pleomorphic adenomas and Warthin's tumours when contrast agents are used [11, 20]. In addition, approaches using computer-aided tissue characterisation are regularly able to differentiate between benign and malignant tumours [13, 21]. However, using these approaches in routine clinical work does not appear feasible yet.

The emergence of sonoelastography as an innovative diagnostic tool for assessing characteristics of different tissues such as their elasticity and stiffness provides an additional method of characterising and thus differentiating between distinct types of parotid lesion [22]. The method involves palpation with an ultrasound probe. A mechanical force (compression or vibration) is applied to the soft tissue, and a conventional ultrasound imaging technique is used to create coloured or grey-scale images showing the deformation of the soft tissue [23]. This innovative ultrasound technique has been successfully used to examine numerous conditions, such as breast cancer [11, 24–26], thyroid nodules [27–31], prostate cancer [32–34] and liver fibrosis [35–37]; and there have only been a few publications on the use of the method in the head and neck region [22, 38, 39].

The aim of the present study was to compare the established sonographical features seen in B-mode and colour-coded Doppler mode for differentiating between malignant and benign parotid tumours, using innovative characteristics defined on sonoelastography. The elastographical data were therefore analysed to identify characteristic patterns, and the usefulness of ultrasound elastography for differentiating between parotid gland tumours in everyday routine work was assessed.

Materials and methods

The 57 patients included in the study were referred to our department with an unclear mass in the parotid gland between December 2008 and March 2010. A complete ultrasound examination of the head and neck region was carried out, including B-mode, colour-coded Doppler mode and elastographical assessment of the tumours. The examinations were performed with an Acuson S 2000 unit equipped with the eSie Touch elastography tool (both Siemens Ltd., Healthcare Sector, Erlangen, Germany) using a 9-MHz linear-array transducer.

The B-mode examination was used to define the following criteria: size and shape of the tumour (round, oval, polycyclic), homogeneous or heterogeneous echotexture, sharp or blurred margins, and presence or absence of distal acoustic phenomena. For this purpose, all of the lesions were examined and measured on two perpendicular planes.

Tumour perfusion was analysed using colour-coded Doppler sonography and classified as either central (hilar), peripheral, diffuse or absent.

Sonoelastography was used to analyse the lesions' stiffness. The same linear-array transducer (9 MHz) was used for B-mode and for elastography assessment. A split-screen mode was chosen to simultaneously display the B-mode and elastography-mode images for the same region. The tumour was centered within the display, and a region of interest (ROI) was set around the lesion, also including some adjacent parotid parenchyma. Subsequently, moderate transducer compression was applied perpendicular to the skin surface. Care was taken to avoid artefacts resulting from sliding of the transducer. The stiffness or elasticity of the tissue can be displayed using a grey scale (white = soft, black = stiff) or a colour scale (purple/blue = soft, green =

medium, yellow/red = stiff), and both scales were applied and documented.

For each tumour, images in B-mode (in two planes) and colour-coded Doppler mode were stored for later interpretation. The elastographical examination was stored as both freeze images and as video clips with the grey-scale and colour-coded scale (four clips per patient with a duration of 10 s each).

The study was designed as a pilot investigation to identify any specific elastographical patterns associated with different histological entities. The interpretation of the examinations was therefore carried out after surgical removal and histopathological analysis of all lesions, so that the histological entity represented by each tumour was known. All of the images and video clips were subsequently reviewed by two experienced ultrasound examiners who were aware of the histological properties of the respective lesions; a consensus opinion was used as the final result.

Statistical analysis included descriptive charts for the patient population, contingency tables using the chi-squared test for the various sonographical and elastographical properties, and a logistic regression model designed to predict malignancy as reliably as possible. The SPSS statistics program was used for statistical analysis (IBM Corporation, Armonk, New York, USA).

Results

Epidemiological and histological data

The study population consisted of 57 patients (30 women, 27 men; age 14–93 years, mean 53.3 years) who all had a diagnosis of a single primary parotid tumour. All of the tumours were removed surgically using parotidectomies of different extents and were examined histopathologically.

The most common histological type was pleomorphic adenoma (38.6%), followed by Warthin's tumour (35.1%) and other benign tumours. Fourteen per cent of the tumours were malignant. The histopathological diagnoses are listed in Table 1.

Table 1 Distribution of histological entities of parotid gland tumours

Histological type	Patients	
	n	%
Benign lesions		
Pleomorphic adenoma	22	38.6
Warthin's tumour	20	35.1
Cystadenoma	2	3.5
Lipoma	2	3.5
Cyst	3	3.5
Malignant lesions		
Squamous cell carcinoma	3	5.3
Mucoepidermoid carcinoma	1	1.8
Salivary duct carcinoma	1	1.8
Basal cell carcinoma	1	1.8
Carcinoma ex pleomorphic adenoma	1	1.8
Metastatic malignant melanoma	1	1.8

Differentiation of benign and malignant tumours: B-mode and elastography

In the next step, the presence of distinct B-mode criteria (echotexture, margin, distal phenomenon) was analysed for benign and malignant lesions, respectively, to identify any significant differences between the two groups; the results are presented in Table 2. Only the margin contour proved to be significantly different, with a sharp margin in benign tumours and a blurred margin in malignancies (P=0.039). This result is not surprising as it reflects the daily clinical experience where benign tumours are well-delineated in different imaging techniques while malignant lesions are predominantly ill-defined and show infiltration of surrounding tissues.

The analysis of the elastographical examinations was aimed at defining and recognising any specific patterns of distribution of stiff and soft areas. The following signs were identified:

- Bull's-eye sign (Fig. 1), with a very soft, ellipsoid area in the centre of a lesion.
- Garland sign (Figs. 2 and 3), with a reticular distribution of stiff tissue within the whole tumour.
- Dense core sign (Figs. 4 and 5), with a central zone of very stiff tissue with softer tissue in the vicinity.
- Half-half sign (Figs. 6 and 7), with a stiff area located in the superficial half of a lesion while the deeper part has a softer appearance.

Table 2 B-mode criteria for benign and malignant parotid tumours

Parameter			*P* value
Echotexture	Homogeneous	Inhomogeneous	1.0
Benign tumours	15	34	
Malignant tumours	3	5	
Contour of margin	Sharp	Blurred	0.039
Benign tumours	46	3	
Malignant tumours	5	3	
Distal acoustic phenomenon	Present	Absent	0.58
Benign tumours	42	5	
Malignant tumours	6	2	

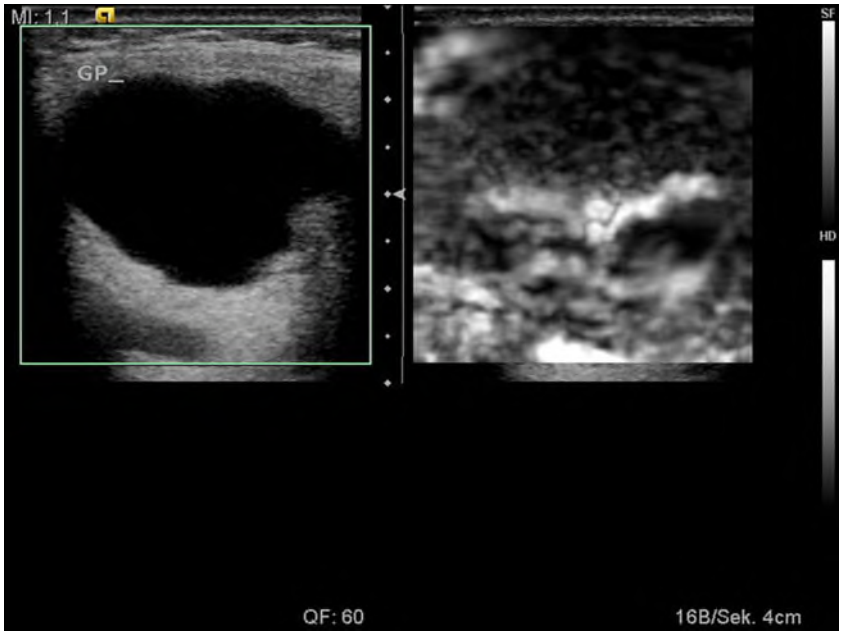

Fig. 1 Split-screen image of a parotid cyst. The B-mode image (*left*) shows the typical hypoechoic homogeneous structure with intense distal acoustic enhancement; the elastography image (*right*) shows the typical configuration of a soft (*white*) horizontal line, resembling a "bull's eye." All of the cysts examined in this study showed the bull's-eye sign

- Soft lesions with harder stripes and tumours with central and peripheral density zones were also found.

The results for the groups of benign and malignant tumours are presented in Table 3.

Analysis of the elastographical criteria showed that the garland sign was present in 3 of 8 malignant tumours (37.5%), but only in 4% (2 of 49) of the benign tumours (Figs. 2 and 3). This difference was statistically significant (P=0.015) denoting that the garland sign appears more frequently in malignant tumours and that its presence may suggest malignancy, especially if additional indicators (e.g. blurred margin) are found. However, it has to be noted that the number of malignant tumours analysed was rather small and that 5 of 8 lesions did not show the garland sign which, thus, does not prove to be as characteristic as desired.

The remaining criteria (e.g. dense core sign, half-half sign) may be more frequent in an individual group (see Table 3), but the differences do not reach statistical significance.

Multivariate analysis and logistic regression model

According to the multivariate analysis of the data (Table 4), a logistic regression model capable of calculating the

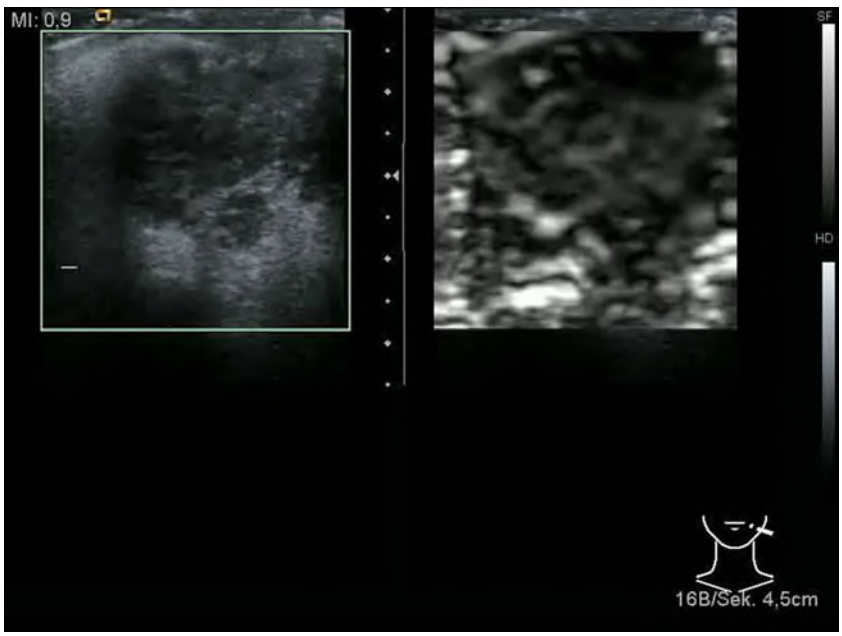

Fig. 2 Split-screen image of a mucoepidermoid carcinoma of the left parotid gland. The B-mode image (*left*) shows a tumour with an irregular shape and blurred margins. The elastography image, displayed with a grey scale (*right*), shows the garland sign, caused by the characteristic distribution of hard (*black*) and soft (*white*) tissue components

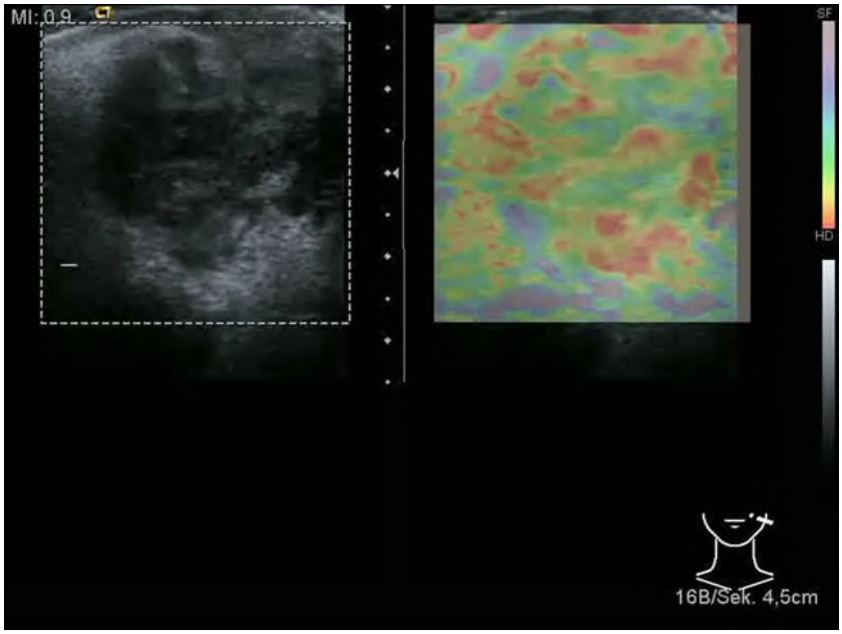

Fig. 3 The corresponding colour-scale elastography image for the malignancy shown in Fig. 2. The garland sign is shown by the *red* reticular structure and represents hard or stiff tissue areas

probability (y) that a parotid lesion is benign as assessed by ultrasonography (with B-mode and elastography combined) is indicated by the following formula: $\log(y/1-y) = 0.079 + 2.374x_1 - 2.793x_2$ where y is the probability that the lesion is benign (1–y: probability that it is malignant); x_1: B-mode→contour of margin (0→sharp; 1→blurred); x_2: elastography→garland sign (0→absent; 1→present).

According to this model, parotid lesions with a sharp margin are more than 10 times more likely to be benign in comparison with lesions with a blurred margin. The probability of a benign entity appears to be only 0.06 times greater in cases with an absent garland sign, although the difference is statistically significant (Table 4). As shown in Table 5, the logistic regression model presented was able to predict that a parotid lesion is benign on the basis of ultrasonographical criteria in 87.7% of the study cases.

Characteristic elastographical patterns of pleomorphic adenomas and Warthin's tumours

The analysis of the elastographic images and video sequences showed that pleomorphic adenomas frequently show the dense core sign (Figs. 4 and 5), while Warthin's tumours

Fig. 4 Split-screen image of a pleomorphic adenoma of the right parotid gland. The B-mode image (*left*) shows an polycyclic, homogeneous, hypoechoic tumour with distal acoustic enhancement. The elastography image shown with a grey scale (*right*) shows a stiffer "sclerotic" central part in the lesion (*black*) with surrounding softer tissue (*white*)—the appearance we have termed "dense core sign"

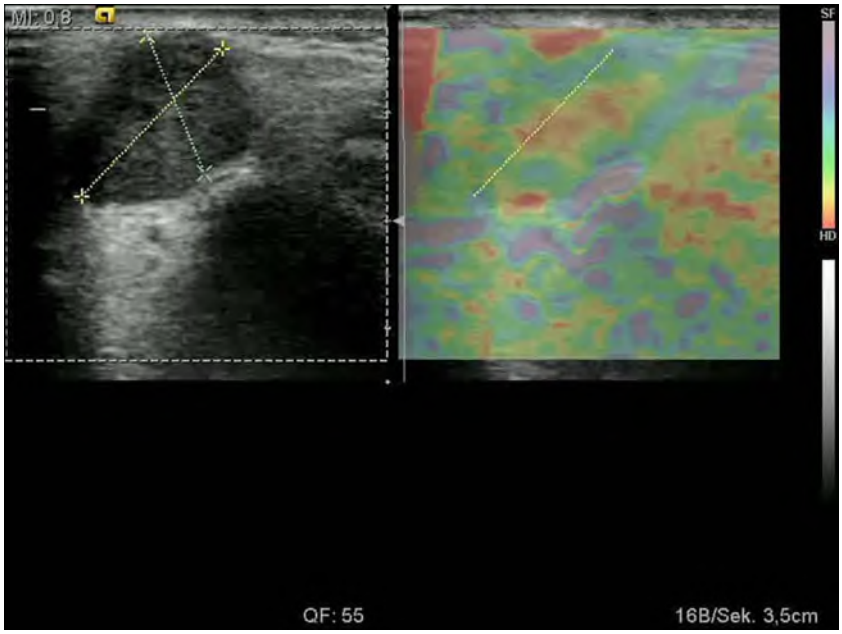

Fig. 5 The corresponding colour-scale elastography image for the pleomorphic adenoma shown in Fig. 4. The dense core sign is shown by the *red* central part, representing the sclerotic core of the tumour, with the surrounding tissue being softer

often present with the half-half sign (Figs. 6 and 7). The statistical significance of this observation was therefore analysed, and it was found that these two elastographical criteria were characteristic patterns in pleomorphic adenomas and Warthin's tumours, respectively, reaching a high level of statistical significance in this context (Tables 6 and 7).

Discussion

The role of imaging in the setting of pretherapeutic tumour diagnosis is not limited to describing the exact location and extent of a given lesion. It can also be used to define the tissue type and assess whether it is benign or malignant as precisely and reliably as possible. With parotid gland tumours, this appears to be a complex task due to the histological variety of both benign and malignant tumours. Numerous approaches have therefore been used in efforts to predict the nature of parotid lesions by defining imaging characteristics, both with ultrasound and CT and MRI, all with limited success [15, 40, 41].

In recent years, sonoelastography has proved to be an important diagnostic tool in assessing the stiffness or elasticity of various tissues [22, 23]. There have been promising

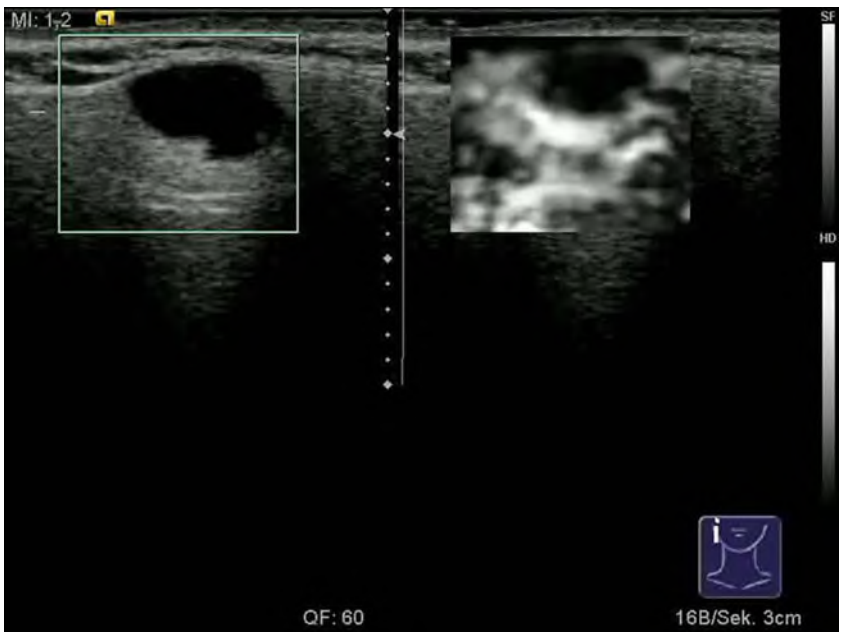

Fig. 6 Split-screen image of a Warthin's tumour in the right parotid gland. The B-mode image (*left*) shows an oval, homogeneous, hypoechoic tumour with distal acoustic enhancement. The elastography image displayed with a grey scale (*right*) shows a division into a stiffer superficial part (*black*) and a softer deep part (*white*)—a typical pattern designated as "half-half sign"

Fig. 7 The corresponding colour-scale elastography image for the Warthin's tumour shown in Fig. 6. The half-half sign is shown by the *red* superficial part and *purple* deep part

results in the diagnosis of breast cancer, thyroid cancer, prostate cancer and liver fibrosis [26, 29, 34, 36]. This raises the question of whether sonoelastography might also be useful in examining parotid gland tumours.

To date, there have only been two published studies on the application of elastography in parotid gland tumours [22, 38]. Bhatia et al. analyzed 65 salivary gland tumours and found that pleomorphic adenomas were significantly firmer or stiffer than Warthin's tumours [38]. As malignancies were also quite stiff on elastographical examination, the study was not able to differentiate sufficiently between benign and malignant tumours. A similar and equally unpromising result was obtained by Dumitriu et al., who analysed 70 salivary gland tumours and found a broad overlap with regard to the elastographical patterns of pleomorphic adenomas and malignancies. The authors concluded that pleomorphic adenomas do not have any specific sonoelastographical characteristics [22]. However, these two studies focus on the lesions' stiffness alone, defining degrees of stiffness or proportions of stiff areas. They do not describe any characteristic configurations of stiff and soft areas within a lesion that can define distinct elastographical patterns.

In the present pilot study, the elastographical examinations were recorded before surgery and analysed afterwards by two experienced ultrasound applicants who were aware of the lesions' histological characteristics. The aim was thus to define specific elastographical patterns with a characteristic distribution of softer and stiffer parts associated with the different parotid gland tumour entities.

The garland sign (Figs. 2 and 3) was successfully identified as a pattern which was found significantly more frequently in malignant (38%) than in benign tumours (4%). It is thus an elastographical feature that may point towards malignancy especially if it coincides with B-mode criteria like a blurred margin and a heterogeneous echotexture. As the multivariate analysis showed, however, it is not a strong criterion in comparison with the blurred margin seen on B-mode ultrasound. A lesion with a blurred margin has a 10-fold higher risk of being malignant than a sharply delineated one, whereas the odds ratio is only 0.06 for the garland sign. Moreover, absence of a garland sign in sonoelastography does not exclude malignancy: 5 of 8 malignant tumours

Table 3 Elastographical criteria for benign and malignant parotid tumours

Parameter			*P* value
Bull's eye sign	Present	Absent	0.548
Benign tumours	5	44	
Malignant tumours	2	6	
Garland sign	Present	Absent	0.015
Benign tumours	2	47	
Malignant tumours	3	5	
Dense core sign	Present	Absent	0.253
Benign tumours	20	29	
Malignant tumours	1	7	
Half-half sign	Present	Absent	0.313
Benign tumours	11	38	
Malignant tumours	0	8	
Soft with harder stripes	Present	Absent	1
Benign tumours	3	46	
Malignant tumours	0	8	
Peripheral and central density zone	Present	Absent	0.365
Benign tumours	10	39	
Malignant tumours	0	8	

Table 4 Multivariate analysis—binary logistic regression

Parameter	B	Odds ratio
Constant	0.079	1.082
Contour of margin	2.374	10.743
Garland sign	−2.793	0.061

analysed in this study did not show this pattern. In conclusion, the garland sign is not as characteristic of malignant tumours as one might desire, but its presence may suggest malignancy as it is found more frequently in malignant tumours and very seldom in benign lesions.

A limitation of the present study is that the number of malignancies included is very small: only eight of 57 parotid tumours proved to be malignant (14%); however, this matches the 10–20% proportion of malignancies in parotid gland tumours reported in the literature. Nevertheless, the number needs to be increased in further studies to improve the statistical performance.

However, it was possible to define a logistic regression model to calculate the probability that a given parotid tumour is benign on the basis of its sonographical and elastographical properties. This is the first time that B-mode ultrasonography and sonoelastography have been combined to predict the malignancy of a parotid lesion.

With regard to the characterisation of the elastographical features of the most common benign parotid gland tumours, this is the first study to describe a specific pattern for both pleomorphic adenomas and Warthin's tumours. The dense core sign (Figs. 4 and 5) was identified as a statistically significant criterion for pleomorphic adenomas, while Warthin's tumours showed the half-half sign (Figs. 6 and 7) as a specific pattern with a high level of statistical significance. Moreover, all of the parotid cysts examined showed the characteristic bull's-eye sign (cf. Fig. 1); however, statistical analysis was not possible here due to the small number of cysts included (three in total). Although these elastographical patterns could not be used to differentiate between benign and malignant tumours, they proved to be characteristic features of a certain histological subgroup of benign parotid gland tumours.

Table 5 Multivariate analysis—predicted and observed rates of benign status in parotid tumours using the logistic regression model

		Observed		Correct prediction	
		Benign	Malignant	*n*	%
Predicted	Benign	47	5	47/52	90.4
	Malignant	2	3	3/5	60
Total		49	8	50/57	87.7

Table 6 Comparison of the dense core sign in pleomorphic adenomas and other parotid tumours

Parameter			*P* value
Dense core sign	Present	Absent	0.000
Pleomorphic adenomas	19	3	
Other tumours	2	33	

The limitations of this pilot study are obvious: the analysis of the data was carried out retrospectively and the examiners were not blinded to the histopathological details of the tumours. Future research will need to include a prospective study and a blinded data analysis. Additionally, the total numbers of cases and in particular the proportion of malignant tumours included need to be increased to improve the statistical power despite the variety of histological subgroups.

Recognising morphological patterns is a qualitative, subjective and observer-dependent method. Conversely, measurements of total or relative tissue stiffness can be used to produce indices and can thus be more objective and better comparable. However, the process may be time-consuming and consequently unsuitable for everyday clinical routine work. Recognising a specific elastographical pattern is fast and does not require any measurements or calculations at all. Familiarity with the patterns that can be found is mandatory, of course. In the present study, a certain learning curve was noted, with pattern recognition improving during the process of data analysis. It will therefore be necessary to train the individual performing the ultrasound examinations, not only in handling the elastography tool, but also in identifying elastographical patterns. In our experience, this process is rapid and easy when there are noticeable and typical patterns such as a garland or a bull's eye.

As the definition of elastographical patterns in this study was carried out on the basis of data obtained with the eSie Touch tool (Siemens Ltd., Healthcare Sector, Erlangen, Germany), there might be some limitations with regard to reproducing these patterns if the examination is carried out with different ultrasound devices. However, it can be expected that the characteristic patterns defined by the tissue distribution are less dependent on a specific software tool than indices or ratios and that they can be recognised more easily even if the colour or other display features vary.

Table 7 Comparison of the half-half sign in Warthin's tumours and other parotid tumours

Parameter			*P* value
Half-half sign	Present	Absent	0.01
Warthin's tumours	8	12	
Other tumours	3	34	

In conclusion, different elastographical patterns (viz: the garland, the dense core, and the half-half sign) are found more frequently in specific histological subtypes of parotid gland tumours. Sonoelastography can therefore improve the diagnostic performance of ultrasound, which is still the most important imaging technique in the assessment of abnormalities in the salivary glands.

Acknowledgements Nils Klintworth and Konstantinos Mantsopoulos contributed equally to this study.

References

1. Stennert E, Wittekindt C, Klussmann JP, Guntinas-Lichius O (2004) New aspects in parotid gland surgery. Otolaryngol Pol 58:109–114
2. Klintworth N, Zenk J, Koch M, Iro H (2010) Postoperative complications after extracapsular dissection of benign parotid lesions with particular reference to facial nerve function. Laryngoscope 120:484–490. doi:10.1002/lary.20801
3. Rehberg E, Schroeder HG, Kleinsasser O (1998) Surgery in benign parotid tumors: individually adapted or standardized radical interventions? Laryngorhinootologie 77:283–288. doi:10.1055/s-2007-996975
4. Zbaren P, Guelat D, Loosli H, Stauffer E (2008) Parotid tumors: fine-needle aspiration and/or frozen section. Otolaryngol Head Neck Surg 139:811–815. doi:10.1016/j.otohns.2008.09.013
5. Howlett DC, Mercer J, Williams MD (2008) Same day diagnosis of neck lumps using ultrasound-guided fine-needle core biopsy. Br J Oral Maxillofac Surg 46:64–65
6. Hausegger KW, Krasa H, Pelzmann W, Grasser RK, Frisch C, Simon H (1993) Sonography of the salivary glands. Ultraschall Med 14:68–74
7. Yasumoto M, Yoshimura R, Sunaba K, Shibuya H (2001) Sonographic appearances of malignant lymphoma of the salivary glands. J Clin Ultrasound 29:491–498
8. Zhang L, Zhang ZY (2010) Evaluation of the ultrasonographic features of salivary gland tumours. Chin J Dent Res 13:133–137
9. Burke CJ, Thomas RH, Howlett D (2010) Imaging the major salivary glands. Br J Oral Maxillofac Surg 49:261–269
10. Thoeny HC (2007) Imaging of salivary gland tumours. Cancer Imaging 7:52–62
11. Wojcinski S, Farrokh A, Weber S et al (2010) Multicenter study of ultrasound real-time tissue elastography in 779 cases for the assessment of breast lesions: improved diagnostic performance by combining the BI-RADS(R)-US classification system with sonoelastography. Ultraschall Med 31:484–491
12. Yonetsu K, Ohki M, Kumazawa S, Eida S, Sumi M, Nakamura T (2004) Parotid tumors: differentiation of benign and malignant tumors with quantitative sonographic analyses. Ultrasound Med Biol 30:567–574
13. Scheipers U, Siebers S, Gottwald F et al (2005) Sonohistology for the computerized differentiation of parotid gland tumors. Ultrasound Med Biol 31:1287–1296
14. Yabuuchi H, Matsuo Y, Kamitani T et al (2008) Parotid gland tumors: can addition of diffusion-weighted MR imaging to dynamic contrast-enhanced MR imaging improve diagnostic accuracy in characterization? Radiology 249:909–916
15. Habermann CR, Arndt C, Graessner J et al (2009) Diffusion-weighted echo-planar MR imaging of primary parotid gland tumors: is a prediction of different histologic subtypes possible? AJNR Am J Neuroradiol 30:591–596
16. Christe A, Waldherr C, Hallett R, Zbaeren P, Thoeny H (2011) MR imaging of parotid tumors: typical lesion characteristics in MR imaging improve discrimination between benign and malignant disease. AJNR Am J Neuroradiol 32:1202–1207
17. Fodor D, Pop S, Maniu A, Cosgaria M (2010) Gray scale and Doppler ultrasonography of the benign tumors of parotid gland (pleomorphic adenoma and Warthin's tumor). Pictorial essay. Med Ultrason 12:238–244
18. Ajayi BA, Pugh ND, Carolan G, Woodcock JP (1992) Salivary gland tumours: is colour Doppler imaging of added value in their preoperative assessment? Eur J Surg Oncol 18:463–468
19. Chikui T, Tokumori K, Yoshiura K, Oobu K, Nakamura S, Nakamura K (2005) Sonographic texture characterization of salivary gland tumors by fractal analyses. Ultrasound Med Biol 31:1297–1304
20. Steinhart H, Zenk J, Sprang K, Bozzato A, Iro H (2003) Contrast-enhanced color Doppler sonography of parotid gland tumors. Eur Arch Otorhinolaryngol 260:344–348
21. Siebers S, Zenk J, Bozzato A, Klintworth N, Iro H, Ermert H (2010) Computer aided diagnosis of parotid gland lesions using ultrasonic multi-feature tissue characterization. Ultrasound Med Biol 36:1525–1534
22. Dumitriu D, Dudea SM, Botar-Jid C, Baciut G (2010) Ultrasonographic and sonoelastographic features of pleomorphic adenomas of the salivary glands. Med Ultrason 12:175–183
23. Hall TJ (2003) AAPM/RSNA physics tutorial for residents: topics in US: beyond the basics: elasticity imaging with US. Radiographics 23:1657–1671
24. Leong LC, Sim LS, Lee YS et al (2010) A prospective study to compare the diagnostic performance of breast elastography versus conventional breast ultrasound. Clin Radiol 65:887–894
25. Schaefer FK, Heer I, Schaefer PJ et al (2011) Breast ultrasound elastography—results of 193 breast lesions in a prospective study with histopathologic correlation. Eur J Radiol 77:450–456
26. Adamietz BR, Meier-Meitinger M, Fasching P et al (2011) New diagnostic criteria in real-time elastography for the assessment of breast lesions. Ultraschall Med 32:67–73
27. Bojunga J, Herrmann E, Meyer G, Weber S, Zeuzem S, Friedrich-Rust M (2010) Real-time elastography for the differentiation of benign and malignant thyroid nodules: a meta-analysis. Thyroid 20:1145–1150
28. Holtel MR (2010) Emerging technology in head and neck ultrasonography. Otolaryngol Clin North Am 43:1267–1274, vii
29. Luo S, Kim EH, Dighe M, Kim Y (2011) Thyroid nodule classification using ultrasound elastography via linear discriminant analysis. Ultrasonics 51:425–431
30. Oliver C, Vaillant-Lombard J, Albarel F et al (2011) What is the contribution of elastography to thyroid nodules evaluation? Ann Endocrinol (Paris) 72:120–124
31. Sporea I, Vlad M, Bota S et al (2011) Thyroid stiffness assessment by acoustic radiation force impulse elastography (ARFI). Ultraschall Med 32:281–285
32. Pinto F, Totaro A, Calarco A et al (2011) Imaging in prostate cancer diagnosis: present role and future perspectives. Urol Int 86:373–382
33. Seitz M, Strittmatter F, Roosen A, Tilki D, Gratzke C (2010) Current status of ultrasound imaging in prostate cancer. Panminerva Med 52:189–194
34. Mahdavi SS, Moradi M, Wen X, Morris WJ, Salcudean SE (2011) Evaluation of visualization of the prostate gland in vibro-elastography images. Med Image Anal 15:589–600
35. Andersen ES, Christensen PB, Weis N (2009) Transient elastography for liver fibrosis diagnosis. Eur J Intern Med 20:339–342
36. Goertz RS, Amann K, Heide R, Bernatik T, Neurath MF, Strobel D (2011) An abdominal and thyroid status with Acoustic Radiation

Force Impulse Elastometry - a feasibility srudy: Acoustic Radiation Force Impulse Elastometry of human organs. Eur J Radiol 80 (3):e226–e230. doi:10.1016/j.ejrad.2010.09.025
37. Heide R, Strobel D, Bernatik T, Goertz RS (2010) Characterization of focal liver lesions (FLL) with acoustic radiation force impulse (ARFI) elastometry. Ultraschall Med 31:405–409
38. Bhatia KS, Rasalkar DD, Lee YP et al (2010) Evaluation of real-time qualitative sonoelastography of focal lesions in the parotid and submandibular glands: applications and limitations. Eur Radiol 20:1958–1964
39. Lyshchik A, Higashi T, Asato R et al (2007) Cervical lymph node metastases: diagnosis at sonoelastography—initial experience. Radiology 243:258–267
40. Bozzato A, Zenk J, Greess H et al (2007) Potential of ultrasound diagnosis for parotid tumors: analysis of qualitative and quantitative parameters. Otolaryngol Head Neck Surg 137:642–646
41. Poorten VV, Hart A, Vauterin T et al (2009) Prognostic index for patients with parotid carcinoma: international external validation in a Belgian–German database. Cancer 115:540–550. doi:10.1002/cncr.24015